J. Fluid Mech. (2007), *vol.* 578, *pp.* 435–451.
doi:10.1017/S0022112007005149 Printed in the United Kingdom

Effective velocity boundary condition at a mixed slip surface

M. SBRAGAGLIA[1] AND A. PROSPERETTI[1,2]

[1]Faculty of Applied Sciences, IMPACT, and Burgerscentrum, University of Twente, AE 7500 Enschede, The Netherlands

[2]Department of Mechanical Engineering, The Johns Hopkins University, Baltimore, MD 21218, USA

(Received 23 June 2006 and in revised form 4 December 2006)

This paper studies the nature of the effective velocity boundary condition for liquid flow over a plane boundary on which small free-slip islands are randomly distributed. It is found that an effective Navier partial-slip condition for the velocity emerges from a statistical analysis valid for arbitrary fractional area coverage β. As an example, the general theory is applied to the low-β limit and this result is extended heuristically to finite β with a resulting slip length proportional to $a\beta/(1-\beta)$, where a is a characteristic size of the islands. A specification of the nature of the free-slip islands is not required in the analysis. They could be nano-bubbles, as suggested by recent experiments, or hydrophobic surface patches. The results are also relevant for ultra-hydrophobic surfaces exploiting the so-called 'lotus effect'.

1. Introduction

The recent blossoming of research in micro-fluidics has prompted renewed interest in the possibility of slip boundary conditions at the contact of a liquid with a solid wall (see e.g. Lauga, Brenner & Stone 2007; Neto *et al.* 2005). While many experiments have provided evidence for a violation of the classical no-slip boundary condition at small spatial scales (e.g. Vinogradova 1999; Watanabe, Yanuar & Udagawa 1999; Pit, Hervet & Léger 2000; Craig, Neto & Williams 2001; Zhu & Granick 2001, 2002; Tretheway & Meinhart 2002; Cheng & Giordano 2002), the physical mechanisms responsible for this phenomenon are still unclear. An interesting possibility is the recent discovery of what appear to be small gas nano-bubbles or pockets attached to the wall (Bunkin *et al.* 1996; Watanabe *et al.* 1999; Ishida *et al.* 2000; Tyrrell & Attard 2001; Holmberg *et al.* 2003; Steitz *et al.* 2003; Simonsen, Hansen & Klösgen 2004; Dammer & Lohse 2006; Sbragaglia *et al.* 2006). The evidence for the existence of these nano-bubbles is somewhat indirect, but nevertheless compelling. It is also hypothesized and, sometimes, experimentally verified (Watanabe *et al.* 1999), that gas pockets may form in cracks or other imperfections of the solid wall, thereby decreasing the overall wall stress.

In order to explore the macroscopic consequences of the existence of such drag-reducing structures on a solid wall – be they gaseous or of another nature – in this study we consider by statistical means the effective velocity boundary condition produced by a random distribution of small free-slip regions on an otherwise no-slip boundary. We consider both the three-dimensional problem, in which the regions are equal disks, and the two-dimensional problem, in which they are strips oriented perpendicularly to the flow. While idealized, these geometries provide some insight into the macroscopic effects of randomly distributed microscopic free-slip regions.

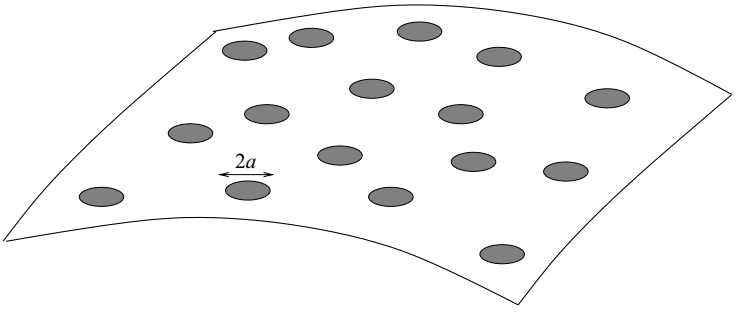

FIGURE 1. Solid no-slip boundary with a random distribution of equal circular free-slip areas.

We find that, away from the wall, the velocity field appears to satisfy a partial-slip condition with the wall velocity linearly related by a possibly non-local operator to the viscous traction at the wall. After deriving this general result, as an example we solve the problem to first order accuracy in the fractional area coverage β. In this limit the relation becomes local and an explicit result for the conventionally defined slip length is derived. The dilute-limit result is extended to finite area fractions by means of a heuristic argument.

As discussed in § 8, our results are consistent with those of a recent paper by Lauga & Stone (2003), who assumed a periodic distribution of free-slip patches on a boundary, as well as those of an older paper by Philip (1972) who similarly investigated the effect of free-slip strips arranged periodically on a plane wall parallel or orthogonal to the direction of the flow.

The present results are also related to the so-called 'lotus effect' (Barthlott & Neinhaus 1997) exploited to obtain ultra-hydrophobic surfaces. Such surfaces are manufactured by covering a solid boundary with an array of hydrophobic micron-size posts which, due to the effect of surface tension, prevent a complete wetting of the wall (see e.g. Ou, Perot & Rothstein 2004; Ou & Rothstein 2005; Choi & Kim 2006; Joseph *et al.* 2006). In the space between the posts the liquid remains suspended away from the wall, with its surface in contact only with the ambient gas, and a concomitant reduction in the mean traction per unit area. Another instance of drag reduction by a similar mechanism has also been reported in Watanabe *et al.* (1999). These authors studied the pressure drop in the flow of a viscous liquid in a tube, the wall of which contained many fine grooves which prevented a complete wetting of the boundary.

The approach used in this paper is mainly suggested by the theory of multiple scattering (see e.g. Foldy 1945; Twersky 1957, 1983) and was used previously to derive the effective boundary conditions at a rough surface for the Laplace and Stokes problems (Sarkar & Prosperetti 1995, 1996). More recent studies devoted to the same problem are the papers by Jäger & Mikelić (2001) and Tartakovsky & Xiu (2006).

2. Formulation

We consider the flow in the neighbourhood of a locally plane boundary† $\mathscr{B}$ with a composite micro-structure which dictates free-slip conditions on certain areas $s^1, s^2, \ldots, s^N$ and no-slip conditions on the remainder $\mathscr{B} - \cup_{\alpha=1}^{N} s^\alpha$ (figure 1). If each

† For the present purposes a curved boundary can be considered plane provided the radius of curvature is large compared with the size of the free-slip regions and their mean reciprocal distance, of order $a/\beta^{1/2}$.

'island' s^α is sufficiently small, and $\cup_{\alpha=1}^{N} s^\alpha$ is also sufficiently small (both in a sense to be made precise later), near the boundary the flow is described by the Stokes equations:

$$\nabla p = \mu \nabla^2 \boldsymbol{u}, \qquad \nabla \cdot \boldsymbol{u} = 0, \tag{2.1}$$

in which p and $\boldsymbol{u}$ are the pressure and velocity fields and μ the viscosity. On the free-slip regions $\boldsymbol{u}$ satisfies the condition of vanishing tangential stress:

$$\boldsymbol{t}_J \cdot (\boldsymbol{\tau} \cdot \hat{\boldsymbol{n}}) = 0, \qquad \boldsymbol{x} \in s^\alpha, \qquad \alpha = 1, 2, \ldots, N, \qquad J = 2, 3, \tag{2.2}$$

where $\boldsymbol{t}_2$ and $\boldsymbol{t}_3$ are two unit vectors in the plane and $\boldsymbol{\tau}$ the viscous stress tensor, while, on the rest of the surface,

$$\boldsymbol{u} = 0, \qquad \boldsymbol{x} \notin \cup_{\alpha=1}^{N} s^\alpha. \tag{2.3}$$

The normal velocity vanishes everywhere on $\mathscr{B}$.

We start by decomposing the solution $(p, \boldsymbol{u})$ as

$$\boldsymbol{u} = \boldsymbol{u}^0 + \sum_{\alpha=1}^{N} \boldsymbol{v}^\alpha, \qquad p = p^0 + \sum_{\alpha=1}^{N} q^\alpha. \tag{2.4}$$

Here $\boldsymbol{u}^0$ and p^0 are the (deterministic) solution satisfying the usual no-slip condition on the entire boundary $\mathscr{B}$ while the fields $(q^\alpha, \boldsymbol{v}^\alpha)$ account for the effect of the αth island. We define these local fields so that $\boldsymbol{v}^\alpha$ vanishes everywhere on $\mathscr{B}$ except on s^α, where it is such that the free-slip condition (2.2) is satisfied. To express this condition it is convenient to define

$$\boldsymbol{w}^\alpha = \boldsymbol{u}^0 + \sum_{\beta \neq \alpha} \boldsymbol{v}^\beta, \qquad r^\alpha = p^0 + \sum_{\beta \neq \alpha} q^\beta, \tag{2.5}$$

so that, for every $\alpha = 1, 2, \ldots, N$,

$$\boldsymbol{u} = \boldsymbol{v}^\alpha + \boldsymbol{w}^\alpha, \qquad p = q^\alpha + r^\alpha. \tag{2.6}$$

On s^α, then, $\boldsymbol{v}^\alpha$ satisfies

$$\boldsymbol{t}_J \cdot (\boldsymbol{\tau}^{v\alpha} \cdot \hat{\boldsymbol{n}}) = -\boldsymbol{t}_J \cdot (\boldsymbol{\tau}^{w\alpha} \cdot \hat{\boldsymbol{n}}), \qquad \boldsymbol{x} \in s^\alpha, \qquad J = 2, 3, \tag{2.7}$$

where

$$\boldsymbol{\tau}^{v\alpha} = \mu[\nabla \boldsymbol{v}^\alpha + (\nabla \boldsymbol{v}^\alpha)^T], \qquad \tau^{w\alpha} = \mu[\nabla \boldsymbol{w}^\alpha + (\nabla \boldsymbol{w}^\alpha)^T], \tag{2.8}$$

the superscript T denoting the transpose. Clearly

$$\boldsymbol{v}^\alpha \to 0, \qquad q^\alpha \to 0 \qquad \text{as} \qquad |\boldsymbol{x} - \boldsymbol{y}^\alpha| \to \infty, \tag{2.9}$$

with $\boldsymbol{y}^\alpha$ a reference point on the αth island. It is evident that both fields $\boldsymbol{v}^\alpha$ and $\boldsymbol{w}^\alpha$ satisfy the Stokes equations. In the terminology of multiple scattering, they are often referred to as the 'scattered' and 'incident' fields, respectively (see e.g. Foldy 1945; Rubinstein & Keller 1989).

3. Averaging

We assume that the free-slip islands are identical circular disks with radius a, centred at $\boldsymbol{y}^\alpha$, with $\alpha = 1, 2, \ldots, N$. We make use of the method of ensemble averaging and consider an ensemble of surfaces differing from each other only in the arrangement of the N free-slip islands. Each arrangement, or configuration, is denoted by

$\mathscr{C}^N = (\boldsymbol{y}^1, \boldsymbol{y}^2, \ldots, \boldsymbol{y}^N)$. A particular configuration will then occur with a probability $P(\mathscr{C}^N) = P(N)$ normalized according to

$$\frac{1}{N!}\int \mathrm{d}^2 y^1 \cdots \int \mathrm{d}^2 y^N P(\boldsymbol{y}^1, \ldots, \boldsymbol{y}^N) \equiv \frac{1}{N!}\int \mathrm{d}\mathscr{C}^N P(N) = 1. \tag{3.1}$$

The ensemble-average velocity is defined as

$$\langle \boldsymbol{u}\rangle(\boldsymbol{x}) = \frac{1}{N!}\int \mathrm{d}\mathscr{C}^N P(N)\, \boldsymbol{u}(\boldsymbol{x}|N) \tag{3.2}$$

where the notation $\boldsymbol{u}(\boldsymbol{x}|N)$ stresses the dependence of the exact field not only on the point $\boldsymbol{x}$, but also on the configuration of the N islands. In view of the fact that $\boldsymbol{u}^0$ is independent of the configuration of the disks, substitution of the decomposition (2.4) into (3.2) gives

$$\langle \boldsymbol{u}\rangle(\boldsymbol{x}) = \boldsymbol{u}^0(\boldsymbol{x}) + \frac{1}{N!}\sum_{\alpha=1}^{N}\int \mathrm{d}\mathscr{C}^N P(N)\, \boldsymbol{v}^\alpha(\boldsymbol{x}|N). \tag{3.3}$$

Since the disks are identical, each one gives the same contribution to the integral. Upon introducing the conditional probability $P(N-1|\boldsymbol{y}^1)$ defined so that $P(N) = P(\boldsymbol{y}^1)\, P(N-1|\boldsymbol{y}^1)$, we may therefore write

$$\langle \boldsymbol{u}\rangle(\boldsymbol{x}) = \boldsymbol{u}^0(\boldsymbol{x}) + \frac{1}{(N-1)!}\int \mathrm{d}\mathscr{C}^N P(\boldsymbol{y}^1)\, P(N-1|\boldsymbol{y}^1)\, \boldsymbol{v}^1(\boldsymbol{x}|\boldsymbol{y}^1, N-1) \tag{3.4}$$

or, in terms of the conditional average

$$\langle \boldsymbol{v}^1\rangle_1(\boldsymbol{x}|\boldsymbol{y}^1) = \frac{1}{(N-1)!}\int \mathrm{d}\mathscr{C}^{N-1} P(N-1|\boldsymbol{y}^1)\, \boldsymbol{v}^1(\boldsymbol{x}|\boldsymbol{y}^1, N-1), \tag{3.5}$$

$$\langle \boldsymbol{u}\rangle(\boldsymbol{x}) = \boldsymbol{u}^0(\boldsymbol{x}) + \int_{\mathscr{B}} \mathrm{d}^2 y\, P(\boldsymbol{y})\, \langle \boldsymbol{v}\rangle_1(\boldsymbol{x}|\boldsymbol{y}), \tag{3.6}$$

where the integral is over the entire boundary. For convenience, here and in the following, we drop the superscript 1 on the quantities referring to disk 1. Since $\boldsymbol{v}^\alpha$ and q^α satisfy the Stokes equations everywhere, so do $\langle \boldsymbol{v}\rangle_1$ and $\langle q\rangle_1$. The boundary conditions are

$$\langle \boldsymbol{v}\rangle_1 = 0, \qquad \boldsymbol{x} \notin s, \tag{3.7}$$

while

$$\boldsymbol{t}_J \cdot (\langle \boldsymbol{\tau}^v\rangle_1 \cdot \hat{\boldsymbol{n}}) = -\boldsymbol{t}_J \cdot (\langle \boldsymbol{\tau}^w\rangle_1 \cdot \hat{\boldsymbol{n}}), \qquad \boldsymbol{x} \in s, \qquad J = 2, 3. \tag{3.8}$$

Note that

$$\langle \tau^w_{jk}\rangle_1 = \mu(\langle \partial_j w_k\rangle_1 + \langle \partial_k w_j\rangle_1) = \mu(\partial_j \langle w_k\rangle_1 + \partial_k \langle w_j\rangle_1), \tag{3.9}$$

and similarly for $\langle \tau^v_{jk}\rangle_1$ since averaging and differentiation commute as is evident from the definition (3.2). The normal velocity vanishes everywhere:

$$\langle v_\perp\rangle_1 \equiv \hat{\boldsymbol{n}} \cdot \langle \boldsymbol{v}\rangle_1 = 0, \qquad \boldsymbol{x} \in \mathscr{B}. \tag{3.10}$$

It may be noted that $P(\boldsymbol{x})$ is just the number density of free-slip islands per unit surface area of the boundary; the area fraction β covered by these islands is

$$\beta(\boldsymbol{x}) = \int_{|\boldsymbol{x}-\boldsymbol{y}|\leqslant a} P(\boldsymbol{y})\, d^2 y \simeq \pi a^2 P(\boldsymbol{x}) + O(a^2/L^2), \tag{3.11}$$

where L, assumed much greater than a, is the characteristic length scale for variations of the number density.

The framework just described can be readily extended to disks of unequal radius, and to non-isotropic islands such as ellipses. In both cases the probability density would depend on a suitably enlarged list of variables such as the disk radius, the characteristic size, orientation and aspect ratio of the ellipses, and so on.

4. The effective boundary condition

Now we derive a formal expression for the effective boundary condition on $\mathscr{B}$. To this end, let $G^W_{ij}(\boldsymbol{y};\boldsymbol{x})$ be the Green's tensor for the Stokes problem, vanishing at infinity and on the plane boundary $\mathscr{B}$. Then

$$\langle v_j\rangle_1(\boldsymbol{x}|\boldsymbol{y}) = \int_{\mathscr{B}} \left[\langle -q\hat{n}_i + (\boldsymbol{\tau}^v\cdot\hat{\boldsymbol{n}})_i\rangle_1(\boldsymbol{s}|\boldsymbol{y})G^W_{ij}(\boldsymbol{s};\boldsymbol{x}) - \langle v_i\rangle_1(\boldsymbol{s}|\boldsymbol{y})T^W_{ijk}(\boldsymbol{s};\boldsymbol{x})n_k\right] \mathrm{d}^2 s, \quad (4.1)$$

where T^W_{ijk} is the stress Green's function associated with G^W_{ij} (see e.g. Kim & Karrila 1991; Pozrikidis 1992) and the integral is extended over the entire plane boundary. This formula can be considerably simplified by recalling that, on the boundary, $\boldsymbol{v}$ vanishes everywhere outside s while G^W vanishes everywhere. Furthermore, on s, the tangential tractions also vanish. Hence, upon taking the x_1-axis along the normal with $x_1 = 0$ on the plane, we have

$$\langle v_j\rangle_1(\boldsymbol{x}|\boldsymbol{y}) = \int_s \langle v_i\rangle_1(\boldsymbol{s}|\boldsymbol{y})T^W_{ij1}(\boldsymbol{s};\boldsymbol{x})\,\mathrm{d}^2 s, \quad (4.2)$$

where now the integration is extended only over the free-slip island. We now consider points $\boldsymbol{x}$ such that $|\boldsymbol{x}-\boldsymbol{s}| \gg a$, but such that $|\boldsymbol{x}-\boldsymbol{s}|$ is sufficiently small to be in the Stokes region adjacent to the boundary. It can be verified that, in this range, we have

$$T^W_{ij1}(\boldsymbol{s};\boldsymbol{x}) = 2T_{ij1}(\boldsymbol{y};\boldsymbol{x})\left[1 + O\left(\frac{a}{|\boldsymbol{x}-\boldsymbol{s}|}\right)\right], \quad (4.3)$$

where T_{ijk} is the free-space stress Green's function:

$$T_{ijk}(\boldsymbol{y};\boldsymbol{x}) = \frac{3}{4\pi}\frac{(y_i-x_i)(y_j-x_j)(y_k-x_k)}{|\boldsymbol{y}-\boldsymbol{x}|^5}. \quad (4.4)$$

Thus, (4.2) becomes

$$\langle v_j\rangle_1(\boldsymbol{x}|\boldsymbol{y}) \simeq -2\pi a^2 T_{ij1}(\boldsymbol{y};\boldsymbol{x})V_i(\boldsymbol{y}), \quad (4.5)$$

where

$$V_i(\boldsymbol{y}) = \frac{1}{\pi a^2}\int_{|s-y|\leqslant a} \langle v_i\rangle_1(\boldsymbol{s}|\boldsymbol{y})\,\mathrm{d}^2 s \quad (4.6)$$

is the average velocity over the disk centred at $\boldsymbol{y}$. Note that $V_1 = 0$ as $v_1 = 0$. This result may now be inserted into the expression (3.6) for the average field to find

$$\langle u_j\rangle(\boldsymbol{x}) = u^0_j(\boldsymbol{x}) - 2\pi a^2 \int \mathrm{d}^2 y\, P(\boldsymbol{y})\, T_{ij1}(\boldsymbol{y};\boldsymbol{x})V_i(\boldsymbol{y}). \quad (4.7)$$

We now take the 'inner limit' of (4.7) by letting the field point $\boldsymbol{x}$ approach $\mathscr{B}$ to find (see e.g. Pozrikidis 1992, pp. 23 and 27)

$$\lim_{x_1\to 0} T_{ij1}(\boldsymbol{y};\boldsymbol{x}) = -\tfrac{1}{2}\delta_{ij}\delta(\boldsymbol{x}-\boldsymbol{y}) \quad (4.8)$$

and recall that $u^0_j(\boldsymbol{x}) = 0$ at the wall so that

$$\langle \boldsymbol{u}_\parallel\rangle(\boldsymbol{x}) = \pi a^2 P(\boldsymbol{x})\,\boldsymbol{V}(\boldsymbol{x}), \quad (4.9)$$

where $\boldsymbol{u}_\parallel$ is the velocity component parallel to the boundary. Since the problem is linear, a dimensionless linear tensor operator W_{ij} must exist such that

$$V_i = \frac{a}{\mu} W_{ij}(\langle \boldsymbol{\tau}^w \rangle_1 \cdot \hat{\boldsymbol{n}})_j \tag{4.10}$$

so that the average field satisfies the partial-slip condition

$$\langle \boldsymbol{u}_\parallel \rangle(\boldsymbol{x}) = \frac{\pi a^3}{\mu} P(\boldsymbol{x}) \boldsymbol{W} \cdot (\langle \boldsymbol{\tau}^w \rangle_1 \cdot \hat{\boldsymbol{n}}) \simeq \frac{a\beta}{\mu} \boldsymbol{W} \cdot (\langle \boldsymbol{\tau}^w \rangle_1 \cdot \hat{\boldsymbol{n}}), \tag{4.11}$$

where the approximate sign is a consequence of equating $\pi a^2 P$ with the area fraction β (see equation (3.11)). This is the main result of this paper, and shows the emergence of a Navier-type mixed-slip effective boundary condition for an arbitrary fraction of the wall surface covered by free-slip patches. It can form the starting point of further analysis or numerical computation. A simple application to the case of small area fraction β will be found in the next section and a heuristic argument for the general case in § 6.

It may be noted that, according to (3.8), $\langle \boldsymbol{v} \rangle_1$ is forced by a generally spatially varying $\langle \boldsymbol{\tau}^w \rangle_1 \cdot \hat{\boldsymbol{n}}$ and, therefore, one may expect the operator $\boldsymbol{W}$ to be non-local. It should also be noted that the term $\langle \boldsymbol{\tau}^w \rangle_1$ appearing here is not the average viscous stress of the total mean flow, to which in general it will be related by a non-necessarily local linear relation. These considerations show that the relation between the wall velocity and viscous traction may be expected to be non-local in general, so that the slip length will be an operator, rather than a scalar quantity. Furthermore, since $\boldsymbol{W}$ is not necessarily an isotropic tensor, in general there is a possibility for $\langle \boldsymbol{u}_\parallel \rangle$ not to be parallel to the local traction at the wall.

We can now be more specific about the assumption made at the beginning of § 2 on the validity of the Stokes equations near the wall. The condition for this assumption is evidently that the Reynolds number

$$Re = \frac{2a|\boldsymbol{V}|}{\nu} \tag{4.12}$$

with ν the kinematic viscosity, be sufficiently small. Equation (4.10) shows that $|\boldsymbol{V}|$ is of the order of a/μ times the magnitude of the wall shear stress; a precise result in a particular case is derived in Appendix A.

5. First-order problem

While exact, the result (4.11) expresses the effective boundary condition on the unconditionally averaged field $\langle \boldsymbol{u} \rangle$ in terms of the conditionally averaged wall stress $\langle \boldsymbol{\tau}^w \rangle_1$. In order to obtain the conditionally averaged velocity $\langle \boldsymbol{u} \rangle_1$ necessary to evaluate this quantity, one would need an effective boundary condition which would involve the wall stress averaged conditionally with the position of two free-slip islands prescribed, and so on. This is the well-known closure problem that arises in ensemble averaging. An explicit solution can only be found by somehow truncating the resulting hierarchy of equations.

The lowest-order non-trivial truncation can be effected with an accuracy of first order in the area fraction β. It is well known that, in this limit, the average 'incident' $\langle \boldsymbol{w} \rangle_1$ may be approximated by the unconditional average $\langle \boldsymbol{u} \rangle$ so that

$$\langle \boldsymbol{u}_\parallel \rangle(\boldsymbol{x}) = \frac{a\beta}{\mu} \boldsymbol{W} \cdot [\langle \boldsymbol{\tau} \rangle(\boldsymbol{x}) \cdot \hat{\boldsymbol{n}}] + o(\beta). \tag{5.1}$$

If the density of the islands is small, since $\boldsymbol{w}$ accounts for the effect of all the other islands on the one centred at $\boldsymbol{y}$, $\langle \boldsymbol{w} \rangle_1$ is slowly varying near $\boldsymbol{y}$ so that

$$\langle \boldsymbol{w} \rangle_1(\boldsymbol{x}) = \langle \boldsymbol{w} \rangle_1(\boldsymbol{y}) + [(\boldsymbol{x} - \boldsymbol{y}) \cdot \nabla] \langle \boldsymbol{w} \rangle_1(\boldsymbol{y}) + \cdots \tag{5.2}$$

and, therefore,

$$\left\langle \tau^w_{jk} \right\rangle_1 = \mu(\partial_j \langle w_k \rangle_1 + \partial_k \langle w_j \rangle_1) \simeq \mu(\partial_j \langle u_k \rangle + \partial_k \langle u_j \rangle) = \langle \tau_{jk} \rangle \tag{5.3}$$

is approximately constant over the island $|\boldsymbol{x} - \boldsymbol{y}| \leqslant a$. The velocity field $\langle \boldsymbol{v} \rangle_1$ is therefore the solution of the Stokes equations (2.1) vanishing at infinity and whose normal component vanishes on the entire plane; the two tangential components vanish for $|\boldsymbol{x} - \boldsymbol{y}| > a$ while, for $J = 2, 3$ and $|\boldsymbol{x} - \boldsymbol{y}| < a$

$$\boldsymbol{t}_J \cdot ([\nabla \langle \boldsymbol{v} \rangle_1 + (\nabla \langle \boldsymbol{v} \rangle_1)^T] \cdot \hat{\boldsymbol{n}}) = -\frac{1}{\mu} \boldsymbol{t}_J \cdot (\langle \boldsymbol{\tau} \rangle \cdot \hat{\boldsymbol{n}}) = \text{const.} \tag{5.4}$$

This problem is solved in the Appendix A where it is shown that

$$W_{ij} = \frac{8}{9\pi} \delta_{ij} \tag{5.5}$$

so that the effective boundary condition (4.11) becomes

$$\langle \boldsymbol{u}_\parallel \rangle(\boldsymbol{x}) = \frac{8}{9\pi} \frac{a}{\mu} \beta(\boldsymbol{x}) (\langle \boldsymbol{\tau} \rangle(\boldsymbol{x}) \cdot \hat{\boldsymbol{n}}) + o(\beta). \tag{5.6}$$

This relation shows that, to the present approximation, the slip length ℓ is given by

$$\ell = \frac{8}{9\pi} \beta \, a. \tag{5.7}$$

It may be expected that, if the islands had an intrinsic direction (e.g. an elliptical shape) and were not randomly oriented, the tensor W_{ij} would not be isotropic so that the average surface traction and surface velocity would not be collinear.

6. A heuristic argument for large area fraction

We now treat in a heuristic manner the non-dilute case of β finite. For this purpose, we imagine that an average partial-slip condition has been established by the presence of many free-slip islands, and we consider the effect of a single free-slip disk on this average field.

Our starting point is equation (4.7) in which now the field $u^0_j(\boldsymbol{x})$ is to be interpreted as the average field, rather than the 'bare' field as before. Now, upon taking the inner limit that led to (4.8), this term will give a β-dependent non-zero contribution $c(\beta)\langle \boldsymbol{u}_\parallel \rangle$ which does not vanish on the wall. In place of (4.9), we thus would find

$$\langle \boldsymbol{u}_\parallel \rangle(\boldsymbol{x}) \; = \; c(\beta) \, \langle \boldsymbol{u}_\parallel \rangle + \pi a^2 P(\boldsymbol{x}) \, \boldsymbol{V}(\boldsymbol{x}). \tag{6.1}$$

By (5.6), this argument leads to the estimate

$$\ell \; \simeq \; \frac{8}{9\pi} \frac{\beta}{1 - c(\beta)} \, a. \tag{6.2}$$

For consistency with the dilute limit of the previous section, we must require that $c(0) = 0$. In the opposite limit $\beta \to 1$, one may expect that ℓ diverges, which is also confirmed by existing analyses (see e.g. Lauga & Stone 2003). The simplest possibility,

which gives the same singular behaviour as found by Lauga & Stone (2003) for large slip lengths, is $c(\beta) = \beta$, with which we have the estimate

$$\ell \simeq \frac{8}{9\pi}\frac{\beta}{1-\beta}\,a. \tag{6.3}$$

An exact result for the non-dilute case can be obtained from the definition (4.10) of the tensor $\boldsymbol{W}$. If in this relation we take $(\langle\boldsymbol{\tau}^w\rangle_1 \cdot \hat{\boldsymbol{n}})_j$ to be a unit vector in each one of the coordinate directions, we are led to the same calculation as carried out in the previous section with the result that W_{ij} acting on a unit vector equals $(8/9\pi)\delta_{ij}$ whatever the fractional area coverage. This result does not necessarily imply that the linear operator $\boldsymbol{W}$ is isotropic, but only that the average of its kernel enjoys this property.

7. The two-dimensional case

A similar analysis can also be applied to the analogous two-dimensional case, i.e. a surface with a random distribution of parallel, or nearly parallel, free-shear strips of width a oriented perpendicular to the flow direction. The developments at the beginning of §4 are still valid and we may start from (4.2) noting that, in place of (4.4), we have

$$T_{ijk}(\boldsymbol{y};\boldsymbol{x}) = \frac{1}{\pi}\frac{(y_i - x_i)(y_j - x_j)(y_k - x_k)}{|\boldsymbol{y}-\boldsymbol{x}|^4}, \tag{7.1}$$

so that (4.2) becomes, in this case,

$$\langle v_j\rangle_1(\boldsymbol{x}|\xi) \simeq 2aT_{j21}(\xi;\boldsymbol{x})V_2(\xi), \tag{7.2}$$

where ξ is the coordinate in the direction parallel to the plane. Here

$$V_2(\xi) = \frac{1}{a}\int_{|\zeta-\xi|\leqslant a} \langle v_2\rangle_1(\zeta|\xi)\,\mathrm{d}\zeta \tag{7.3}$$

is again the average velocity over the strip centred at ξ. The expression (3.6) for the average field is modified to

$$\langle u_j\rangle(\boldsymbol{x}) = u_{0j}(\boldsymbol{x}) + 2a\int \mathrm{d}\xi\; P(\xi)\,T_{j21}(\xi;\boldsymbol{x})V_2(\xi). \tag{7.4}$$

The analogue of (4.8) is still valid so that

$$\langle u_2\rangle(\xi) = a\,P(\xi)\,V_2(\xi), \tag{7.5}$$

where u_2 is the velocity component parallel to the boundary.

As before, from the linearity of the problem we deduce the existence of a dimensionless quantity W such that

$$V = \frac{a}{\mu}W\langle\tau^w_{xy}\rangle_1 \tag{7.6}$$

so that the average field satisfies the partial-slip condition

$$\langle u\rangle(\xi) = \frac{a}{\mu}\beta(\xi)W\langle\tau^w_{xy}\rangle_1, \tag{7.7}$$

where we have used the fact that the fraction of the boundary covered by the free-slip strips is now given by

$$\beta(\xi) = \int_{|\zeta-\xi|\leqslant a} P(\zeta)\,\mathrm{d}\zeta \simeq aP(\xi) + O(a^2/L^2). \tag{7.8}$$

The solution of the problem in the dilute limit is given in Appendix B. One finds

$$W = \frac{\pi}{16} \tag{7.9}$$

so that the effective boundary condition becomes

$$\langle u \rangle(\xi) = \frac{\pi}{16} \frac{a}{\mu} \beta(\xi) \langle \tau_{xy} \rangle + o(\beta). \tag{7.10}$$

Arguments similar to those presented in § 6 permit us to extend this dilute-limit case to finite β with the result

$$\ell = \frac{\pi}{16} \frac{\beta}{1-\beta} a, \tag{7.11}$$

8. Conclusions

We have shown that an effective Navier partial-slip condition for the velocity on a wall covered by a random arrangement of free-slip disks or two-dimensional strips emerges from a statistical analysis. For the case of disks we have proposed for the slip length ℓ the relation

$$\ell = \frac{8}{9\pi} \frac{\beta}{1-\beta} a, \tag{8.1}$$

where a is the common radius of the disks. The first-order result $\ell = (8/9\pi)\beta a$ derives from a rigorous calculation given in § 5. The finite-β correction in the denominator derives from heuristic considerations.

These expressions have been obtained by starting from a rigorous result, given in equation (4.11), which is of general validity and can be used to obtain closures based on numerical simulations. As argued in § 4, one may expect that, in a correct theory, the slip length will be a non-local linear operator rather than a scalar.

One of the motivations of this study was the possibility that gaseous structures attached to the solid wall, such as nano-bubbles, could furnish a mechanism explaining the partial slip observed by several investigators and it is therefore interesting to examine how the result (8.1) compares with available data.

The study of Simonsen *et al.* (2004) quotes $a \simeq 75\,\text{nm}$ and $\beta \simeq 60\,\%$. With these values, the estimate (8.1) gives $\ell \simeq 32\,\text{nm}$. This value for the slip length is similar to that measured by several investigators, such as Zhu & Granick (2002), who report $0 \leqslant \ell < 40\,\text{nm}$ for water, and Craig *et al.* (2001), who report $0 \leqslant \ell < 18\,\text{nm}$, for water–sucrose solutions.

Wu *et al.* (2005) measure a very low nano-bubble number density of about 3 bubbles per $10\,\mu\text{m}^2$, with typical radii of the order of 100 nm, which gives $\beta \simeq 1\,\%$ and $\ell \simeq 0.3\,\text{nm}$. This is small, but not out of line with some of the existing measurements.

The radius of surface nano-bubbles reported by Holmberg *et al.* (2003) is in the range 25 to 65 nm while that reported by Ishida *et al.* (2000) is of the order of 300 nm. With an area coverage of 20 %, we can estimate a slip length between about 2 and 20 nm. Again, these numerical values are in the expected range.

Tyrrell & Attard (2001) and Steitz *et al.* (2003) measure an area coverage of the order of 90 %. With $a = 10$ and 100 nm, our heuristic result (8.1) gives slip lengths of 25 and 250 nm, respectively. Unfortunately, neither group measured the slip length.

Tretheway & Meinhart (2002) measured a slip length of about 1 μm, but made no estimates of area coverage or free-slip patch size. With $\ell = 1\,\mu\text{m}$ and $\beta \sim 50\,\%$, (8.1) gives a bubble radius $a = 3.53\,\mu\text{m}$. This is another case for which it would be of great interest to have some information on the surface structures.

The free-slip islands in Watanabe *et al.*'s (1999) work were cracks with a width of about 10 μm and a length of the order 100 μm. If an equivalent radius is estimated as $\pi a^2 = 10 \times 100\,\mu\text{m}^2$, one finds $a \simeq 18\,\mu$m. In this case, as already found by Lauga & Stone (2003), one would need a large value of β to recover the slip length of 450 μm estimated by the authors.

According to Craig *et al.* (2001), the slip length is a function of the shear stress. Zhu & Granick (2002) find a threshold value of the flow rate for the appearance of a slip effect. These are inherently nonlinear results, which cannot be captured by a linear model such as the one we study which, by its very nature, is only applicable for small shear.

It is also of interest to compare our results with those of Lauga & Stone (2003) obtained for flows in a tube with a periodic arrangement of free-slip rings perpendicular to the flow. For large tube radius, this arrangement should be comparable to our two-dimensional analysis. For the general case, their solution is numerical, but they provide an approximate analytic expressions valid for large tube radius, namely

$$\ell = \frac{H}{2\pi} \log\left(\sec\left(\frac{\pi}{2}\beta\right)\right), \tag{8.2}$$

where H is the spatial period. Upon expanding for small β, we find

$$\ell \simeq \frac{\pi}{16} H\beta^2, \tag{8.3}$$

which, with the identification $H\beta = a$, is in precise agreement with our two-dimensional result (7.10). Lauga & Stone (2003) also give a similar result for free-slip strips parallel to the flow, but this situation is not comparable with either of the two that we have considered.

We are indebted with Dr S. M. Dammer for directing us to many pertinent references. M. S. is grateful to Professor D. Lohse for several enlightening discussions and to STW (Nanoned Programme) for financial support.

Appendix A. Solution of the three-dimensional problem

We take the centre of the island as the origin, with the z-axis normal to the plane and the x-axis parallel to the tangential component of the traction $\langle\boldsymbol{\tau}\rangle\cdot\boldsymbol{n}$. Since the normal velocity component vanishes, with this choice of coordinates we require

$$\frac{\partial v_x}{\partial z} = S, \qquad \frac{\partial v_y}{\partial z} = 0, \tag{A 1}$$

where

$$S = -\frac{1}{\mu}(\langle\boldsymbol{\tau}\rangle\cdot\boldsymbol{n})_x. \tag{A 2}$$

Here and in the following we write $\boldsymbol{v}$ in place of $\langle\boldsymbol{v}\rangle_1$ for convenience. Furthermore we measure lengths with respect to the island radius a, although no special notation will be used to indicate dimensionless variables. It is convenient to adopt a system of cylindrical coordinates (r, θ, z) in which $v_x = v_r\cos\theta - v_\theta\sin\theta$, $v_y = v_r\sin\theta + v_\theta\cos\theta$, in terms of which the condition (A 1) becomes

$$\frac{\partial v_r}{\partial z} = S\cos\theta, \qquad \frac{\partial v_\theta}{\partial z} = -S\sin\theta. \tag{A 3}$$

Following Ranger (1978) (see also Smith 1987; Davis 1991; Stone & Ajdari 1998), we represent the velocity field in the form

$$\boldsymbol{v} = \nabla \times \left[\frac{\sin\theta}{r} \chi(r,z)\hat{\boldsymbol{e}}_z + \nabla \times \left(\frac{\cos\theta}{r} \psi(r,z)\hat{\boldsymbol{e}}_z \right) \right] \tag{A 4}$$

where $\hat{\boldsymbol{e}}_z$ is a unit vector normal to the plane and

$$\mathrm{L}\chi = 0 \qquad \mathrm{L}^2\psi = 0 \tag{A 5}$$

with

$$\mathrm{L} = \frac{\partial^2}{\partial r^2} - \frac{1}{r}\frac{\partial}{\partial r} + \frac{\partial^2}{\partial z^2}. \tag{A 6}$$

The Cartesian velocity components follow from (A 4) as

$$v_x(r,z,\theta) = \frac{1}{2} r \partial_r \left[\frac{1}{r^2} (\partial_z \psi - \chi) \right] \cos 2\theta + \frac{1}{2r} \partial_r (\partial_z \psi + \chi), \tag{A 7}$$

$$v_y(r,z,\theta) = \frac{1}{2} r \partial_r \left[\frac{1}{r^2} (\partial_z \psi - \chi) \right] \sin 2\theta, \tag{A 8}$$

$$v_z(r,z,\theta) = -\partial_r \left(\frac{1}{r} \partial_r \psi \right) \cos\theta, \tag{A 9}$$

while, from the Stokes equation, the pressure is found as

$$p(r,z,\theta) = \mu \frac{\cos\theta}{r} \frac{\partial}{\partial z} \mathrm{L}\psi. \tag{A 10}$$

The solution of (A 5) is sought in the form of Hankel transforms with the result

$$\psi = rz \int_0^\infty \mathrm{e}^{-kz} J_1(kr) \tilde{\psi}(k)\, \mathrm{d}k, \tag{A 11}$$

$$\chi = r \int_0^\infty \mathrm{e}^{-kz} J_1(kr) \tilde{\chi}(k)\, \mathrm{d}k. \tag{A 12}$$

The functions $\tilde{\psi}$ and $\tilde{\chi}$ must be determined by imposing the boundary conditions. Upon substituting (A 11) and (A 12) into (A 7) and (A 8), we find that the no-slip condition outside the disk is satisfied provided that

$$\int_0^\infty J_1(kr) \left(\tilde{\psi}(k) + \tilde{\chi}(k) \right) \mathrm{d}k = \frac{d}{r}, \qquad r > 1, \tag{A 13}$$

$$\int_0^\infty J_1(kr) \left(\tilde{\psi}(k) - \tilde{\chi}(k) \right) \mathrm{d}k = 0, \qquad r > 1, \tag{A 14}$$

where d is an integration constant to be determined later. The stress condition (A 1) inside the disk is satisfied provided that

$$\int_0^\infty J_1(kr) \left(-2\tilde{\psi}(k) - \tilde{\chi}(k) \right) k\, \mathrm{d}k = Sr, \qquad 0 < r < 1, \tag{A 15}$$

$$\int_0^\infty J_1(kr) \left(-2\tilde{\psi}(k) + \tilde{\chi}(k) \right) k\, \mathrm{d}k = br, \qquad 0 < r < 1, \tag{A 16}$$

where b is another integration constant. Upon adding and subtracting, we find two pairs of dual integral equations for $\tilde{\psi}$ and $\tilde{\chi}$:

$$\int_0^\infty J_1(kr)\tilde{\psi}(k)\,\mathrm{d}k = \frac{d}{2r}, \qquad 1 < r, \tag{A 17}$$

$$\int_0^\infty J_1(kr)\tilde{\psi}(k)k\,\mathrm{d}k = -\frac{1}{4}(b+S)r, \qquad 0 < r < 1, \tag{A 18}$$

and

$$\int_0^\infty J_1(kr)\tilde{\chi}(k)\,\mathrm{d}k = \frac{d}{2r}, \qquad 1 < r, \tag{A 19}$$

$$\int_0^\infty J_1(kr)\tilde{\chi}(k)k\,\mathrm{d}k = \frac{1}{2}(b-S)r, \quad 0 < r < 1. \tag{A 20}$$

Both these problems have the standard Titchmarsh form

$$\int_0^\infty J_1(kr)\tilde{c}(k)\,\mathrm{d}k = \frac{B}{r}, \qquad 1 < r, \tag{A 21}$$

$$\int_0^\infty J_1(kr)\tilde{c}(k)k\,\mathrm{d}k = Ar, \qquad 0 < r < 1, \tag{A 22}$$

the solution of which is (see e.g. Sneddon 1966, p. 84):

$$\tilde{c} = \frac{2}{3}\sqrt{\frac{2}{\pi}}A\frac{J_{5/2}(k)}{\sqrt{k}} + B\frac{\sin k}{k}. \tag{A 23}$$

With this result the Hankel transforms can be evaluated in their complementary intervals finding

$$\int_0^\infty J_1(kr)\tilde{c}(k)k\,\mathrm{d}k = \left(B - \frac{4A}{3\pi}\right)\frac{1}{r\sqrt{r^2-1}} - \frac{4A}{2\pi r}\left[\sqrt{r^2-1} - r^2\arcsin\left(\frac{1}{r}\right)\right], \quad r > 1, \tag{A 24}$$

$$\int_0^\infty J_1(kr)\tilde{c}(k)\,\mathrm{d}k = \frac{4}{3}\frac{A}{\pi}r\sqrt{1-r^2} + B\frac{1-\sqrt{1-r^2}}{r}, \quad 0 < r < 1. \tag{A 25}$$

For both expressions to be regular at $r = 0$ it is necessary that

$$B = \frac{4A}{3\pi}. \tag{A 26}$$

Upon imposing this condition on the solutions for $\tilde{\psi}$ and $\tilde{\chi}$ we find

$$d = -\frac{8}{9\pi}S, \qquad b = \frac{1}{3}S \tag{A 27}$$

so that, finally,

$$\tilde{\psi} = \tilde{\chi} = -\frac{4S}{3\sqrt{2\pi}}\frac{J_{3/2}(k)}{\sqrt{k}} = \frac{4S}{3\pi}\frac{k\cos k - \sin k}{k^3}. \tag{A 28}$$

The velocity field inside the disk is readily calculated from these expressions, giving

$$v_x(r,0,\theta) = -\frac{4S}{3\pi}\sqrt{1-r^2}, \qquad v_y(r,0,\theta) = 0. \tag{A 29}$$

The average velocity over the disk is found from direct integration:

$$\frac{1}{\pi}\int_0^{2\pi} \mathrm{d}\theta \int_0^1 r\,\mathrm{d}r\, v_x(r,0,\theta) = -\frac{8S}{3\pi}\int_0^1 r\sqrt{1-r^2}\,\mathrm{d}r = -\frac{8}{9\pi}S, \tag{A 30}$$

while the y component vanishes. Although not necessary for the solution of the problem at hand, it may be of interest to also show explicitly the expressions for the velocity and pressure fields away from the disk. With the definitions:

$$\ell_1 = \frac{1}{2}[\sqrt{(r+1)^2+z^2} - \sqrt{(r-1)^2+z^2}], \tag{A 31}$$

$$\ell_2 = \frac{1}{2}[\sqrt{(r+1)^2+z^2} + \sqrt{(r-1)^2+z^2}], \tag{A 32}$$

the integrals can be evaluated to find (see Gradshteyn & Ryzhik 2000, sections 6.621, 6.751 and 6.752)

$$v_x(r,z,\theta) = -\frac{2Sz}{3\pi}r^2\frac{\sqrt{\ell_2^2-1}}{(\ell_2^2-\ell_1^2)\ell_2^4}\cos 2\theta - \frac{4S}{3\pi}\left(\sqrt{1-\ell_1^2} - z\arcsin\left(\frac{1}{\ell_2}\right)\right) - \frac{2Sz}{3\pi}\left(\frac{\sqrt{\ell_2^2-1}}{(\ell_2^2-\ell_1^2)} - \arcsin\left(\frac{1}{\ell_2}\right)\right), \tag{A 33}$$

$$v_y(r,z,\theta) = -\frac{2Sz}{3\pi}r^2\frac{\sqrt{\ell_2^2-1}}{(\ell_2^2-\ell_1^2)\ell_2^4}\sin 2\theta, \tag{A 34}$$

$$v_z(r,z,\theta) = \frac{4Sz}{3\pi}\left(-\frac{\ell_1^2\sqrt{1-\ell_1^2}}{(\ell_2^2-\ell_1^2)r}\right)\cos 2\theta, \tag{A 35}$$

$$p(r,z,\theta) = \frac{8S\mu}{3\pi}\left(-\frac{\ell_1^2\sqrt{1-\ell_1^2}}{(\ell_2^2-\ell_1^2)r}\right)\cos 2\theta. \tag{A 36}$$

Appendix B. Solution of the two-dimensional problem

In this case it is convenient to adopt as fundamental length $\frac{1}{2}a$ and a Cartesian system of coordinates with x along the flow direction and y along the normal. The boundary conditions of the Stokes problem for v_x and v_y become

$$v_x(x,0) = 0, \qquad |x| > 1, \tag{B 1}$$

$$\partial_y v_x(x,0) = S, \qquad |x| < 1, \tag{B 2}$$

$$v_y(x,0) = 0, \qquad -\infty < x < \infty, \tag{B 3}$$

where

$$S = -\frac{1}{\mu}\langle\tau_{xy}\rangle. \tag{B 4}$$

We introduce a stream function ψ in terms of which

$$v_x(x,y) = \partial_y\psi, \qquad v_y(x,y) = -\partial_x\psi \tag{B 5}$$

and

$$\omega = \partial_y v_x - \partial_x v_y = \nabla^2\psi. \tag{B 6}$$

The vorticity ω is harmonic and can be written as a Fourier integral in the form

$$\omega(x, y) = \int_{-\infty}^{\infty} \mathrm{d}k \exp(\mathrm{i}kx)\tilde{\omega}(k)\mathrm{e}^{-|k|y}. \tag{B 7}$$

By introducing the Fourier transform $\tilde{\psi}(k, y)$ of the stream function, substituting into (B 6), and integrating, we find

$$\tilde{\psi}(k, y) = -\frac{y\tilde{\omega}(k)}{2|k|}\mathrm{e}^{-|k|y} \tag{B 8}$$

after elimination of an integration constant on the basis of (B 3). With this result, the boundary condition (B 1) becomes

$$\int_{-\infty}^{\infty} \mathrm{d}k \exp(\mathrm{i}kx)\tilde{\omega}(k) = S, \qquad |x| < 1, \tag{B 9}$$

and (B 2)

$$\int_{-\infty}^{\infty} \mathrm{d}k \exp(\mathrm{i}kx)\frac{\tilde{\omega}(k)}{|k|} = 0, \qquad |x| > 1. \tag{B 10}$$

Upon writing (B 9) for x and $-x$ and adding or subtracting, we find

$$\int_{-\infty}^{\infty} \mathrm{d}k \cos(kx)\tilde{\omega}(k) = S, \qquad 0 < x < 1, \tag{B 11}$$

$$\int_{-\infty}^{\infty} \mathrm{d}k \sin(kx)\tilde{\omega}(k) = 0, \qquad 0 < x < 1. \tag{B 12}$$

Proceeding in a similar way with (B 10) we have

$$\int_{-\infty}^{\infty} \mathrm{d}k \cos(kx)\frac{\tilde{\omega}(k)}{|k|} = 0, \qquad 1 < x, \tag{B 13}$$

$$\int_{-\infty}^{\infty} \mathrm{d}k \sin(kx)\frac{\tilde{\omega}(k)}{|k|} = 0, \qquad 1 < x. \tag{B 14}$$

If in (B 11) we separate the integration range into $-\infty < k < 0$ and $0 < k < \infty$ we find

$$\int_{0}^{\infty} \mathrm{d}k \cos(kx)\tilde{\omega}_+ = S, \qquad 0 < x < 1, \qquad \tilde{\omega}_+ = \tilde{\omega}(k) + \tilde{\omega}(-k), \tag{B 15}$$

whereas (B 12) gives

$$\int_{0}^{\infty} \mathrm{d}k \sin(kx)\tilde{\omega}_- = 0, \qquad 0 < x < 1, \qquad \tilde{\omega}_- = \tilde{\omega}(k) - \tilde{\omega}(-k). \tag{B 16}$$

Similarly

$$\int_{0}^{\infty} \mathrm{d}k \cos(kx)\frac{\tilde{\omega}_+}{k} = 0, \qquad 1 < x, \tag{B 17}$$

$$\int_{0}^{\infty} \mathrm{d}k \sin(kx)\frac{\tilde{\omega}_-}{k} = 0, \qquad 1 < x. \tag{B 18}$$

Since the problem for $\tilde{\omega}_-$ is completely homogeneous, this quantity must vanish so that $\tilde{\omega}(k)$ is even in k and, therefore, real. We are thus led to the pair of dual integral equations

$$\int_{0}^{\infty} \mathrm{d}k \cos(kx)\tilde{\omega} = \tfrac{1}{2}S, \qquad 0 < x < 1, \tag{B 19}$$

$$\int_0^\infty \mathrm{d}k \cos(kx)\frac{\tilde{\omega}}{k} = 0, \qquad 1 < x. \tag{B 20}$$

This is a standard problem with the solution (see e.g. Sneddon 1966, p. 84)

$$\tilde{\omega}(k) = \tfrac{1}{2} S J_1(k) \tag{B 21}$$

from which the velocity on the boundary follows as

$$v_x(x, 0) = -\frac{S}{2}\cos(\arcsin x) = -\frac{S}{2}\sqrt{1 - x^2}, \qquad x < 1, \tag{B 22}$$

so that

$$\frac{1}{2}\int_{-1}^{1} v_x(x, 0)dx = -\frac{\pi}{8}S. \tag{B 23}$$

This result coincides with that derived by different means in Philip (1972). As before, it may be of some interest to show the explicit results for the velocity and pressure fields. One has

$$v_x(x, y) = -\frac{S}{2}\int_{-\infty}^{\infty} \mathrm{d}k \cos(kx)\left(\frac{1}{|k|} - y\right)\tilde{\omega}(k)\,\mathrm{e}^{-|k|y}, \tag{B 24}$$

$$v_y(x, y) = -\frac{S}{2}\int_{-\infty}^{\infty} \mathrm{d}k \sin(kx) y\tilde{\omega}(k)\,\mathrm{e}^{-|k|y}, \tag{B 25}$$

$$p(x, y) = -2S\int_{0}^{\infty} \mathrm{d}k \sin(kx)\tilde{\omega}(k)\,\mathrm{e}^{-ky}. \tag{B 26}$$

The integrals can be evaluated to find

$$v_x(x, y) = -\frac{S}{2}R(x, y) - \frac{yS}{2}\partial_y R(x, y), \tag{B 27}$$

$$v_y(x, y) = \frac{yS}{2}\partial_y I(x, y), \tag{B 28}$$

$$p(x, y) = S\partial_y R(x, y), \tag{B 29}$$

with

$$R(x, y) = -y + \sqrt{\frac{(1 - x^2 + y^2) + \sqrt{(1 - x^2 + y^2)^2 + 4x^2y^2}}{2}}, \tag{B 30}$$

$$I(x, y) = x + \sqrt{\frac{-(1 - x^2 + y^2) + \sqrt{(1 - x^2 + y^2)^4 + 4x^2y^2}}{2}}. \tag{B 31}$$

REFERENCES

Barthlott, W. & Neinhaus, C. 1997 Purity of the sacred lotus, or escape from contamination in biological surfaces. *Planta* **202**, 1–8.

Bunkin, N. F., Kochergin, A. V., Lobeyev, A. V., Ninham, B. W. & Vinogradova, O. I. 1996 Existence of charged submicrobubble clusters in polar liquids as revealed by correlation between optical cavitation and electrical conductivity. *Colloid Interface Sci.* A **110**, 207–212.

Cheng, J.-T. & Giordano, N. 2002 Fluid flow through nanometer-scale channels. *Phys. Rev. Lett.* **65**, 031206.

Choi, C. H. & Kim, C. J. 2006 Large slip of aqueous liquid flow over a nanoengineered superhydrophobic surface. *Phys. Rev. Lett.* **96**, 066001.

Craig, V. S. J., Neto, C. & Williams, D. R. M. 2001 Shear-dependent boundary slip in an aqueous Newtonian liquid. *Phys. Rev. Lett.* **87**, 054504.

Dammer, S. M. & Lohse, D. 2006 Gas enrichment at liquid-wall interfaces. *Phys. Rev. Lett.* **96**, 206101.

Davis, A. M. J. 1991 Shear flow disturbance due to a hole in the plane. *Phys. Fluids* A **3**, 478–480.

Foldy, L. 1945 The multiple scattering of waves. *Phys. Rev.* **67**, 107–119.

Gradshteyn, I. S. & Ryzhik, I. M. 2000 *Table of Integrals, Series, and Products*, 6th edn. Academic.

Holmberg, M., Kühle, A., Garnaes, J., Mørch, K. A. & Boisen, A. 2003 Nanobubble trouble on gold surfaces. *Langmuir* **19**, 10510–10513.

Ishida, N., Inoue, T., Miyahara, M. & Higashitani, K. 2000 Nano-bubbles on a hydrophobic surface in water observed by tapping-mode atomic force microscopy. *Langmuir* **16**, 6377–6380.

Jäger, W. & Mikelić, A. 2001 On the roughness-induced effective boundary conditions for an incompressible viscous flow. *J. Diffl Equat.* **170**, 96–122.

Joseph, P., Cottin-Bizonne, C., Benoit, J.-M., Ybert, C., Journet, C., Tabeling, P. & Bocquet, L. 2006 Slippage of water past superhydrophobic carbon nanotube forests in microchannels. *Phys. Rev. Lett.* **97**, 156104.

Kim, S. & Karrila, S. 1991 *Microhydrodynamics*. Butterworth-Heinemann.

Lauga, E., Brenner, M. P. & Stone, H. A. 2007 Microfluidics: the no-slip boundary condition. In *Handbook of Experimental Fluid Dynamics* (ed. J. Foss, C. Tropea & A. Yarin). Springer (to appear).

Lauga, E. & Stone, H. A. 2003 Effective slip in pressure-driven Stokes flow. *J. Fluid Mech.* **489**, 55–77.

Neto, C., Evans, D. R., Bonaccurso, E., Butt, H. J. & Craig, V. S. J. 2005 Boundary slip in Newtonian liquids: a review of experimental studies. *Rep. Prog. Phys.* **68**, 2859–897.

Ou, J., Perot, B. & Rothstein, P. 2004 Laminar drag reduction in microchannels using ultrahydrophobic surfaces. *Phys. Fluids* **16**, 4635–4643.

Ou, J. & Rothstein, P. 2005 Direct velocity measurement of the flow past drag-reducing ultrahydrophobic surfaces. *Phys. Fluids* **17**, 103606.

Philip, J. R. 1972 Flows satisfying mixed no-slip and no-shear conditions. *Z. Angew. Math. Phys.* **23**, 353–370.

Pit, R., Hervet, H. & Léger, L. 2000 Direct experimental evidence of slip in hexadecane: Solid interfaces. *Phys. Rev. Lett.* **85**, 980–983.

Pozrikidis, C. 1992 *Boundary Integral and Singularity Methods for Linearized Viscous Flow*. Cambridge University Press.

Ranger, K. B. 1978 The circular disc straddling the interface of a two phase flow. *Intl J. Multiphase Flow* **4**, 263–277.

Rubinstein, J. & Keller, J. 1989 Sedimentation of a dilute suspension. *Phys. Fluids* A **1**, 637–643.

Sarkar, K. & Prosperetti, A. 1995 Effective boundary conditions for the Laplace equation with a rough boundary. *Proc. R. Soc. Lond.* A **451**, 425–452.

Sarkar, K. & Prosperetti, A. 1996 Effective boundary conditions for Stokes flow over a rough surface. *J. Fluid Mech.* **316**, 223–240.

Sbragaglia, M., Benzi, R., Biferale, L., Succi, S. & Toschi, F. 2006 Surface roughness-hydrophobicity coupling in microchannel and nanochannel flows. *Phys. Rev. Lett.* **97**, 204503.

Simonsen, A. C., Hansen, P. L. & Klosgen, B. 2004 Nanobubbles give evidence of incomplete wetting at a hydrophobic interface. *J. Colloid Interface Sci.* **273**, 291–299.

Smith, S. H. 1987 Stokes flows past slits and holes. *Intl J. Multiphase Flow* **13**, 219–231.

Sneddon, I. N. 1966 *Mixed Boundary Value Problems in Potential Theory*. North-Holland.

Steitz, R., Gutberlet, T., Hauss, T., Klösgen, B., Krastev, R., Schemmel, S., Simonsen, A. C. & Findenegg, G. H. 2003 Nanobubbles and their precursor layer at the interface of water against a hydrophobic substrate. *Langmuir* **19**, 2409–2418.

Stone, H. A. & Ajdari, A. 1998 Hydrodynamics of particles embedded in a flat surfactant layer overlying a subphase of finite depth. *J. Fluid Mech.* **369**, 151–173.

Tartakovsky, D. M. & Xiu, D. B. 2006 Stochastic analysis of transport in tubes with rough walls. *J. Comput. Phys.* **217**, 248–259.

Tretheway, D. & Meinhart, C. 2002 Apparent fluid slip at hydrophobic microchannel walls. *Phys. Fluids* **14**, L9–L12.

Twersky, V. 1957 On scattering and reflection of sound by rough surfaces. *J. Acoust. Soc. Am.* **29**, 209–225.

Twersky, V. 1983 Reflection and scattering of sound by correlated rough surfaces. *J. Acoust. Soc. Am.* **73**, 85–94.

Tyrrell, J. W. G. & Attard, P. 2001 Images of nanobubbles on hydrophobic surfaces and their interactions. *Phys. Rev. Lett.* **87**, 176104.

Vinogradova, O. I. 1999 Slippage of water over hydrophobic surfaces. *Intl J. Mineral Proc.* **56**, 31–60.

Watanabe, K., Yanuar & Udagawa, H. 1999 Drag reduction of Newtonian fluid in a circular pipe with a highly water-repellent wall. *J. Fluid Mech.* **381**, 225–238.

Wu, Z., Zhang, X., Zhang, X., Li, G., Sun, J., Zhang, M. & Hu, J. 2005 Nanobubbles influence on BSA adsorption on mica surface. *Surface Interface Anal.* **37**, 797–801.

Zhu, Y. & Granick, S. 2001 Rate-dependent slip of Newtonian liquid at smooth surfaces. *Phys. Rev. Lett.* **87**, 096105.

Zhu, Y. & Granick, S. 2002 Limits of the hydrodynamic no-slip boundary condition. *Phys. Rev. Lett.* **88**, 106102.